Eur. Phys. J. D **7**, 351–359 (1999)

THE EUROPEAN PHYSICAL JOURNAL D

EDP Sciences

Improving the specularity of magnetic mirrors for atoms

G. Zabow[a], M. Drndić, J.H. Thywissen, K.S. Johnson[b], R.M. Westervelt, and M. Prentiss

Department of Physics, Harvard University, Cambridge, Massachusetts 02138, USA

Received 16 November 1998

Abstract. An array of anti-parallel current-carrying wires creates an inhomogeneous magnetic field capable of reflecting neutral atoms. We present analytical and numerical analyses of the magnetic field produced by such an array, and describe methods for reducing the resulting rms angular deviation from specular reflection to less than 0.1 mrad. Careful choice of cross-sectional wire profiles is shown to dramatically improve specularity of reflection close to the surface. Additionally, we find that the specularity depends on whether the number of wires in the mirror is even or odd, and that there exists an optimal turning height above the surface that maximizes the specularity of reflection from the mirror.

PACS. 03.75.Be Atom and neutron optics – 32.80.Pj Optical cooling of atoms; trapping – 85.70.Ay Magnetic device characterization, design, and modeling

1 Introduction

Highly specular mirrors for neutral atoms [1] may be important elements of atom interferometers [2], resonators [3,4] and lasers [5]. Several atomic mirrors have already been suggested and demonstrated [6–10]. In particular, several groups have already either reflected [11–16] or deflected [17,18] neutral atoms using a potential proportional to a magnetic field (B-field) magnitude that decays exponentially as a function of distance from a surface. Such a field can be produced by an alternating surface magnetization or by a set of alternating parallel lines of current [10,19]. However, physical realizations of such arrays also exhibit some periodic modulation in the B-field magnitude in any plane parallel to the surface. This modulation introduces an effective roughness to the mirror by creating equipotential surfaces of constant B-field magnitude that are no longer flat parallel planes. In this paper we consider ways to minimize this unwanted roughness in the equipotentials produced by an array of alternating magnetizations.

The equipotential roughness depends both on the finite mirror size and on the exact spatial magnetization of the alternating magnetic domains or the cross-sectional profiles of the current-carrying wires. For an infinite mirror with an ideal surface "magnetization profile" (produced by either alternating magnetic domains or current-carrying wires), the equipotentials would indeed be perfectly flat; however, for any other magnetization profile this is no longer true. Fortunately, as distance from the surface increases, the exact surface magnetization profile is of lesser physical significance and the roughness in the field of an infinite mirror decreases accordingly. Since the height at which an atom will bounce increases with increasing B-field strength, specularity of reflection from an infinite mirror could be maximized by maximizing the B-field magnitude. However, for any finite mirror this is not true because of additional contributions to the roughness from finite-size edge effects. We show that even at heights comparable to the period of the mirror and much smaller than the mirror length or width, these edge effects dominate and lead to a roughness which increases as a function of height above the mirror. Significantly, the transition to these finite-size effects can occur around the height at which atoms dropped from a magneto-optic trap (MOT) will be reflected. It is therefore important to incorporate such effects into any treatment of the roughness of the effective reflecting surface. Unlike an infinite mirror, we find that a real finite mirror has an optimal finite current/surface magnetization magnitude that reflects the atoms near the height where the equipotentials are flattest. For many configurations, this optimal surface magnetization magnitude is weaker than the maximum field strength realizable experimentally [20].

In this paper we modify the existing theory of an infinite mirror [10,19], incorporating finite-size effects that explain the existence of this optimal turning height. We consider the case of current-carrying wires (although clear analogues exist for permanent magnetic mirrors too) and present ways to flatten the equipotentials on both sides of this optimal turning point, increasing the specularity of reflection and the range of incident atomic velocities that can simultaneously be reflected with high specularity.

[a] e-mail: gary@atomsun.harvard.edu

[b] *Present address*: IGEN International Inc., 16020 Industrial Drive, Gaithersburg, MD 20877, USA.

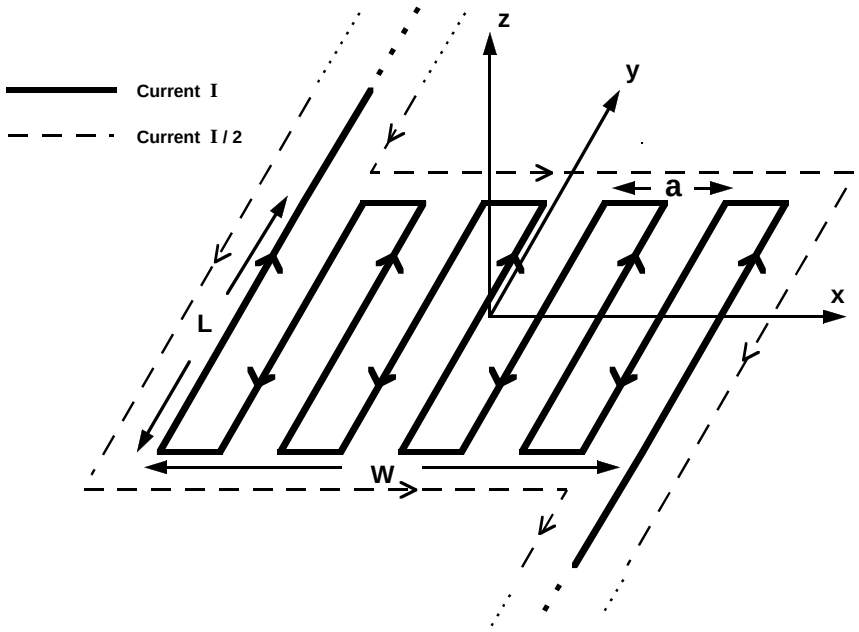

Fig. 1. Schematic of an electromagnet mirror of width W, line length L and periodicity a. The solid line carries the main mirror current I. The dotted lines, carrying a current of $I/2$, show a compensating scheme to minimize effects of the mirror's finite size and of the perturbing magnetic fields of the connecting current leads (see Sect. 3.4).

We start by discussing equipotential surfaces produced at various heights above the mirror. Close to the surface, realistic variations in the cross-sectional wire profile are shown to result in equipotentials orders of magnitude flatter than those produced using either rectangular or circular wire cross-sections [21]. Slightly further from the surface, we investigate the nature of the finite-size induced roughness, and show how to smooth the potentials using compensating wires at the mirror edges as first suggested by Sidorov *et al.* [14]. In addition, we present alternative ways to model the finite-size influences revealing an even/odd parity effect in the number of current lines constituting the mirror [20].

We conclude by presenting numerical simulations of semi-classical atom trajectories through the reflecting B-field potential of a finite-sized mirror. For typical current-carrying magnetic mirror devices reflecting atoms dropped from a MOT, optimizations should be able to reduce the rms angular deviation from specular reflection to less than 0.1 mrad.

2 Mirror definitions and basic principles

We begin by describing a typical micro-electromagnet mirror [16,17]. The bulk of the mirror is constructed from one continuous wire looped back and forth to create a parallel series of wire segments through which the current-flow direction alternates (see Fig. 1). The fundamental spatial period of the mirror, a, is twice the wire separation, since neighbouring wires carry opposing currents. Axes are defined such that x is perpendicular to the long wire direction, y is parallel to it, and z is perpendicular to the $x-y$ mirror plane. The mirror width in the x-direction is defined as W and the mirror length in the y-direction as L. The x and y origins define the mirror centre and z measures the distance from the top of the wires.

The theory of the exponentially decaying B-field above an infinite set of identical alternating currents/magnetic domains [10,19] yields a magnetic scalar potential which we write in the form:

$$\phi_M = \sum_{n=0}^{\infty} \phi_n \cos(nkx)\mathrm{e}^{-nkz}, \qquad z \geq 0 \tag{1}$$

where $k = 2\pi/a$ is the decay constant associated with the fundamental harmonic of period a, and where we have set all phase angles to zero by symmetry. The coefficients in (1) derive from the Fourier series describing the magnetic scalar potential immediately above the wires at $z = 0$, which is itself determined by the current density as a function of both x and z in the wires ($z < 0$). All $\phi_{n=\mathrm{even}} = 0$, since the current flow alternates directions and is necessarily of the same magnitude throughout the mirror series circuit. Additionally, the high harmonics (with their associated rapidly decaying exponentials) decay to negligible levels even a fraction of a decay length above the surface.

If the atomic magnetic moment adiabatically follows the local B-field direction, then the field magnitude determines the reflecting potential [22]. Approximating the surface field magnitude as $B_0 = k\phi_1$, the field magnitude, B, can be approximated as

$$B \approx B_0\mathrm{e}^{-kz}\Big(1 + b_3\mathrm{e}^{-2kz}\cos(2kx) + (\text{terms involving } b_5, b_7 \ \ldots\ )\Big) \tag{2}$$

where the b_3, b_5, $b_7 \ldots$ coefficients are functionals of the current density distribution given by $b_{2n+1} = (2n+1)\phi_{2n+1}/\phi_1$, and are respectively associated

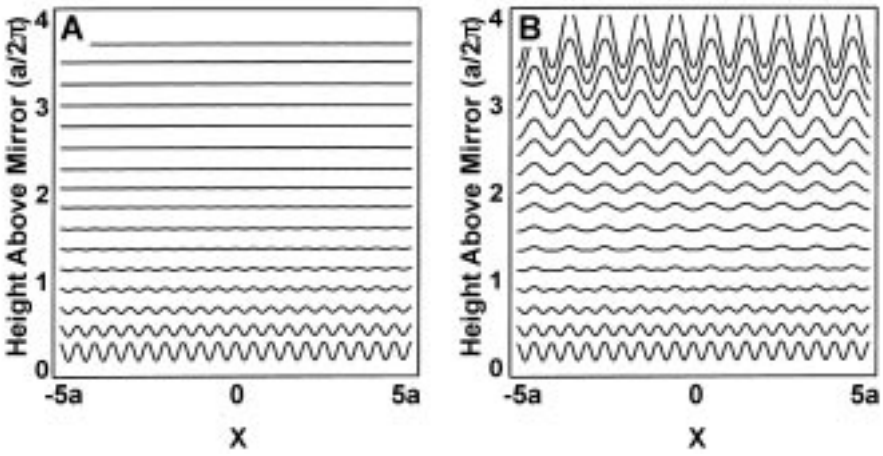

Fig. 2. Absolute magnetic field contour lines (iso-potentials), equi-spaced in z, above (A) a mirror having an infinite number of current-carrying lines and (B) the centre of a finite mirror having 100 lines. The finite mirror iso-potentials become rougher less than two decay lengths above the surface and have dominant periodicity twice that of the iso-potentials above the infinite mirror.

with $\cos(2nkx)$ terms arising from cross terms between the (odd) harmonics.

Equation (2) assumed an infinite array of current-carrying lines. For a finite-sized mirror, this approximation can only be valid within some small distance above the mirror centre. An immediate upper-bound on this distance is obtained by noting the height at which the addition of one extra wire to the mirror edge adds a field of comparable magnitude to the infinite mirror's field. Introducing I for the current, N for the number of lines constituting the mirror, defined by $N = (2W/a) + 1$, and μ_0 for the free-space permeability, this height is approximated by:

$$kz_{\text{finite}} = \ln\left[\frac{\pi B_0}{\mu_0 I} W\right] = \ln\left[\frac{\pi^2 \phi_1}{\mu_0 I} N\right] \approx \ln(N) \qquad (3)$$

where the logarithmic dependence results from the exponentially decaying mirror field being compared to the $1/r$ decay of a single line. For typical wire profiles, $\pi^2\phi_1/\mu_0 I$ is approximately 1.5. In contrast, the mirror size, reflected by the $\ln(N)$ (or equivalently, $\ln(W)$) term, can vary more widely and dominates for typical mirrors having, say, 100 to 1000 lines. The approximate range for z_{finite} is therefore 5 to 7 decay lengths, approximately coinciding with the mirror periodicity a [23].

As an immediate example of this transition from an infinite to finite system, we consider a finite number of lines, each of infinite extent in the y-direction [24]. Figures 2A and 2B show calculated B-field equipotentials at various distances above a mirror with an infinite number of lines (Fig. 2A) and above a mirror with 100 lines (Fig. 2B). The mirror's finite size quickly results in iso-potentials that become rougher with distance from the surface and that have periodicity twice that predicted for an infinite mirror.

3 Improving the specularity of a finite mirror

In this section we explain the fields of Figures 2A and 2B and further analyze the B-field of a realizable finite-sized mirror, presenting means to improve the specularity of the resulting reflection from it. To this end, it is convenient to distinguish three approximate height regimes which we label as the "infinite mirror region" ($z \lesssim a/2$), "finite mirror region" ($z \approx a$), and "mirror far-field region" ($z \gtrsim 2a$), recognizing that their true boundaries are slowly varying functions of the mirror geometry. The lower two regions are seen in Figure 2B, with the transition between them occurring at the height where the equipotentials are flattest. The "mirror far-field region" occurs off the top of the plot, but we note that it too occurs long before the distance from the mirror is even on the order of the mirror width, W.

3.1 "Infinite mirror region"

Close to the surface, equipotential roughness is dominated by the Fourier components determining the magnetic scalar potential which leads to the $b_3, b_5, b_7 \ldots$ coefficients describing the B-field in (2). The higher frequency components decay quickly such that a few decay lengths from the surface, the B-field retains an x-dependence proportional only to $\cos(2kx)$. This exponential decay of the modulating roughness in the B-field suggests that minimal roughness will be obtained for maximal current, since maximizing the field strength maximizes the height at which the atom is reflected above the surface. This strategy is correct only for an infinite mirror; for a finite mirror the roughness does not decrease monotonically with increasing B-field strength (see Fig. 2).

However, the roughness can be alternatively reduced by appropriately changing the cross-sectional wire profiles to reduce the Fourier coefficients appearing

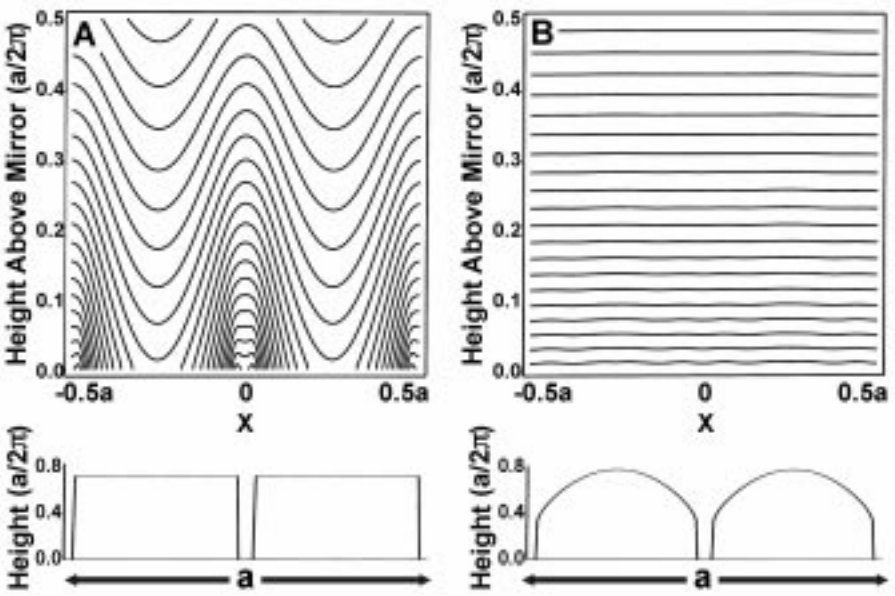

Fig. 3. Absolute magnetic field contours (iso-potentials), equi-spaced in B, above the surface of a mirror having wires of (A), a rectangular, and (B), an optimized cross-sectional profile. The optimized profile shown, yields iso-potentials two orders of magnitude flatter than does the rectangular profile.

in equation (2). We expect the current density in the small (μm scale) mirror wires to be essentially uniform throughout the wire [25], so the current distribution is equated with the wire's cross-section. Recalling that $\mathbf{B} = -\boldsymbol{\nabla}\phi_M$, (1) shows that all b_3, b_5, b_7 ... terms in (2) could be eliminated if a suitable wire profile could be found having a scalar potential immediately above the wires consisting of only the fundamental harmonic. Determining this ideal shape analytically is complicated by the current flow dependence on both x and z positions, the constraint of insulating adjacent wires from each other, and the requirement of ensuring manufacturable wire profiles.

We have found, numerically, that simple profile changes can result in large reductions in the b_3, b_5, b_7 ... coefficients (see Eq. (2)) compared to those resulting for either rectangular or circular cross-sectional wires. Figure 3 shows a comparison between the B-field iso-potentials resulting from wires of rectangular cross-section and from wires of a cross-sectional shape determined by our optimization algorithm. The gain in flatness shown is two orders of magnitude.

Achieving such gains in practice requires precise control over the fabrication process. However, calculations show that even unoptimized rounded wire shapes offer substantial improvements over rectangular wires. By appropriately adjusting processing parameters [17], we have manufactured a variety of "oval-shaped" wires with the best thus far giving calculated iso-potential lines approximately an order of magnitude flatter than those of rectangular wires. Such improvements more than compensate for any decreased current capacity of the wires due to their slightly reduced cross-sectional area as compared to rectangular wires.

3.2 "Finite mirror region"

As distance above the mirror surface increases, the exponentials associated with the Fourier components described above (Sect. 3.1) decay, while the deviations from an infinite mirror become more pronounced, rendering the infinite-mirror treatment invalid. Equation (3) indicated only an upper bound for this infinite-finite transition height. A similar, more accurate calculation [23] shows that for a typical mirror of about 100 lines, the transition point can occur already within the first few decay lengths above the surface, which is typically where cooled atoms dropped a few cm above an electromagnet mirror would be reflected. Additionally, as even (3) shows, the transition height depends only logarithmically on the number of mirror lines. Therefore, for finite-size effects to be completely negligible in typical atom-dropping experiments, the number of current lines would need to be vastly increased, ideally exponentially. Instead, we consider alternative ways to reduce the magnitude of this edge-induced roughness.

Sidorov *et al.* [14] have already made the clever suggestion of using compensating elements, which we call "endcaps", at the edges of a magnetic mirror to simulate a larger mirror. Their idea is to add single extra magnetic elements, or analogously, current carrying wires, at the mirror edges to mimic the B-field that would be contributed if there were alternating magnetic domains/current carrying wires continuing out to infinity. The field at the centre of the mirror is well approximated if the extra wires carry half the current of the other wires in the mirror. At positions away from the centre of the mirror, the agreement is less exact, but in all regions of interest above the mirror it remains a good vector approximation.

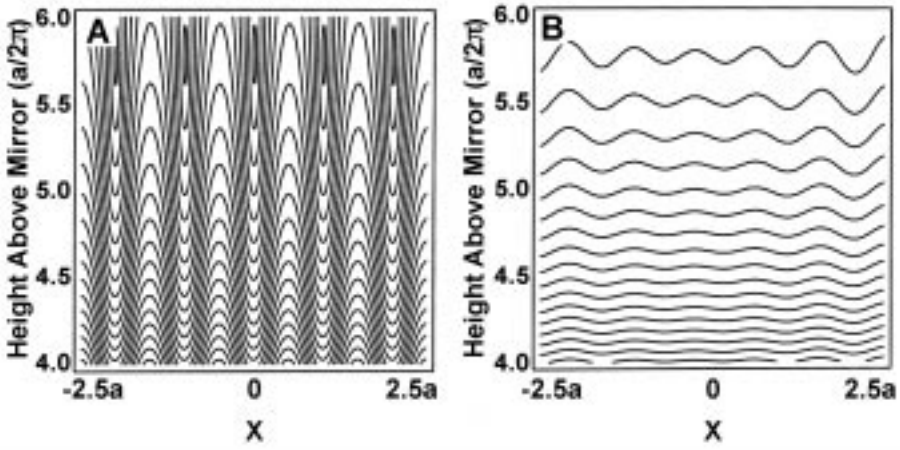

Fig. 4. Absolute magnetic field contours (iso-potentials), equi-spaced in B, above the centre of a mirror with an even (100) number of current-carrying lines (A), and with an odd (101) number of current-carrying lines (B), showing an even-odd parity influence on mirror roughness.

We emphasize that a current line, in particular, approximately corrects the vector B-field everywhere far in from the mirror edge. To first order, this can be understood by grouping the semi-infinite plane of missing wires (extending off from the mirror x-edge to infinity) into a single "monopole" half-wire, closest to the actual mirror edge, and a repeating infinite series of "quadrupole" half-whole-half-wire triplets. Since the infinite sum of "quadrupole" terms gives an a/r^2 fall off in contrast to the $1/r$ decaying field of the residual half-current line, the half-line's B-field dominates at all positions above the mirror that are an appreciable distance ($r \gg a$) in from the edge.

Noting that endcaps provide a good correction in all regions of interest, we choose now to use the complement of these correcting endcaps in constructing an analytic model of a finite-sized mirror. We approximate the difference between the fields of a finite and of an infinite mirror as the negative of the endcaps that would have been added to the finite mirror x-edges to approximately correct it. We call this negative of the endcaps, the "error field", and we then approximate the finite mirror as equivalent to the error field added to an infinite mirror.

Such a model enables both qualitative and quantitative explanations of differences between the finite and infinite systems. For example, consideration of the error field shows that a mirror with an odd number of wires has flatter iso-potentials near its centre than does a mirror with an even number of wires. The composite error field of any mirror is the sum of the two error fields from the mirror's two edges. An odd (even) mirror's edge error currents flow in the same (opposite) direction and therefore, at the mirror centre in the height region in which atoms are reflected, the error fields cancel (add). Since this error field interferes with the infinite mirror harmonics, an even mirror has rougher equipotentials than does an equivalent odd mirror. Even if endcaps are included to correct the finite mirrors to first (or second) order [26], an even mirror will still have a second (or third) order error field while an odd mirror will not. Figure 4 shows a numerical calculation for the B-field iso-potential surfaces above two identical mirrors except that in (A) the mirror has an even number of lines while in (B) it has an odd number.

Since roughness due to finite-size edge effects appears already just a few decay lengths above the surface, equation (2) has only a small region of validity. This region can be extended (to all three height regions) by vectorially adding the error B-field from the mirror's edge error currents to the equation. The error B-field, $\mathbf{B}_{\mathrm{e}}(x,z)$, resolved into x and z components, is:

$$|B_{\mathrm{e}}^{x}(x,z)| = c_{\mathrm{err}} z \left| \frac{1}{r_1^2} \pm \frac{1}{r_2^2} \right|, \qquad z > 0$$
$$|B_{\mathrm{e}}^{z}(x,z)| = c_{\mathrm{err}} \left| \frac{W/2 - x}{r_1^2} \mp \frac{W/2 + x}{r_2^2} \right| \tag{4}$$

where the upper (lower) sign refers to an odd (even) mirror, the constant $c_{\mathrm{err}} = \mu_0 I_{\mathrm{err}}/2\pi$, and r_1 and r_2 are the distances from the point (x,z) to the two missing lines. The modified equation is obtained by first adding these components to the B_x and B_z components obtained from taking appropriate derivatives of (1), before the B-field magnitude is obtained as in (2). Noting that finite-size induced roughness occurs a few decays lengths from the surface, only the first and third harmonics of the infinite mirror field are included giving the approximation:

see equation (5) below

$$B \approx B_0 \mathrm{e}^{-kz} \sqrt{1 + 2b_3 \mathrm{e}^{-2kz} \cos(2kx) + 2\mathrm{e}^{kz} \left(\frac{B_{\mathrm{e}}(x,z)}{B_0} \right) \cos(kx - \theta) + \mathrm{e}^{2kz} \left(\frac{B_{\mathrm{e}}(x,z)}{B_0} \right)^2} \tag{5}$$

where $\theta \equiv \theta(x,z) = \arctan(B_{\rm e}^x(x,z)/B_{\rm e}^z(x,z))$. We note that the third and fourth terms rapidly dominate over the second, and that the third term has twice the periodicity of the second. Unlike an infinite mirror where as distance from the surface is increased (2) predicts a dominant roughness of periodicity $a/2$, a finite mirror instead switches over to a dominant roughness term with period a (see Fig. 2). Note that this periodicity occurs even if $\phi_2 = 0$.

As z increases further through the region $z \approx a$, the second term, the dominant roughness term for an infinite mirror, soon becomes negligible. At these heights, on the curved surface $z(x)$ defined by the solution of $B_{\rm e}(x,z) = B_0 \exp(-kz)$, (5) reduces to a perfect square giving:

$$B(x,z(x)) = 2B_0 {\rm e}^{-kz(x)} \left|\cos\left(\frac{kx-\theta}{2}\right)\right| . \qquad (6)$$

Therefore, in addition to having period a (correct to within the slight modifying factor from the non-constant phase angle θ), the B-field exhibits zero's lying with this periodicity on the surface $z(x)$. That is, there exists a series of local minima in the absolute B-field, that repeat every a in the x-direction and extend in the y-direction forming a set of parallel waveguides. Using (4), the surface $z(x)$ valid near the mirror centre is:

$$\begin{aligned} z(x) &\approx z_{\rm finite} + \frac{1}{k}\ln\left[\frac{W}{2\sqrt{x^2+z^2(x)}}\right] \quad \text{ODD} \\ z(x) &\approx z_{\rm finite} \qquad\qquad\qquad\qquad\quad \text{EVEN} \end{aligned} \qquad (7)$$

where $z_{\rm finite}$ is that calculated in (3). As expected, the zero's are closer to the surface for an even mirror than for an odd one, again indicating that the even mirror is the rougher. These surfaces, derived from the modified B-field equation (5), are in excellent agreement with full numerical calculations of the fields of finite-sized mirrors.

3.3 "Mirror far-field region"

Slightly higher above the mirror, $z \gtrsim 2a$, the error field dominates completely, reducing (5) to $B = B_{\rm e}(x,z)$. This is equivalent to replacing the mirror (either even or odd) by the two edge error currents carrying half the mirror current, in analogy with the replacing of a dielectric by two surface polarization charges. Only at far greater distances where $z \gg W$ (and therefore in regions where the atoms are unlikely ever to be), will the uncorrected odd and even mirrors have substantially different far-field behaviours, the odd mirror appearing as a net flow of current.

3.4 Stray fields

Stray magnetic fields (even spatially uniform ones) are additional sources of roughness since they can produce interference terms with the infinite mirror field harmonics [10]. Indeed, finite size effects, including the doubling in dominant roughness periodicity, the even-odd parity effect, and the repeating waveguide-like minima in the B-field, can all be viewed as consequences of vectorially adding the infinite mirror field to a particular form of stray field: the error field, $\mathbf{B}_{\rm e}(x,z)$, given in (4).

A small uniform stray field, $\mathbf{B}_{\rm s} \equiv B_{\rm s}^x\hat{\mathbf{x}} + B_{\rm s}^z\hat{\mathbf{z}}$, added to a flat infinite mirror, introduces ripples in the isopotentials with slopes ${\rm d}z/{\rm d}x \equiv -(\partial B/\partial x)/(\partial B/\partial z)$ varying sinusoidally with amplitude $(B_{\rm s}/B_0)\exp(kz)$, ($B_{\rm s} \ll B_0$). For example, for $B_0 \approx 100$ G, maintaining flatness of order 0.1 mrad at $kz = 2$, requires shielding against any $B_{\rm s}$ down to ~ 1 mG. Therefore, all possible experimental stray fields having components in the x- or z-directions, should be minimized.

Apart from externally generated stray fields, additional intrinsic stray fields result from the current-carrying mirror itself [27]. One of these is the roughness contribution due to the turning (connecting) sections of wire at the mirror y-edges (see Fig. 1). They provide essentially a piecewise-defined current flow, perpendicular to the major mirror line direction, with magnitude alternating between the mirror current magnitude, I, and zero. This configuration can be regarded as the superposition of a steady current line of $I/2$ and a set of adjacent current pieces alternating between $+I/2$ and $-I/2$. Each piece in this set of alternating current pieces contributes a magnetic field, but their net field rapidly decays in from the mirror edge, effectively leaving only a single line at each y-edge of the mirror with current $I/2$. To approximate its effect on the overall B-field, we assume the B-field to be otherwise perfectly smooth. Adding these two edge line fields to the first harmonic of the infinite mirror field gives the iso-potential slope, ${\rm d}z/{\rm d}x$, valid near the mirror centre:

$$\frac{{\rm d}z}{{\rm d}x} = \frac{2y\mu_0 I \sin(kx){\rm e}^{kz}}{\pi L^2 B_0}\frac{W}{\sqrt{W^2+L^2}} . \qquad (8)$$

This effect is reduced by adding endcaps along the mirror y-edges (much like the x-edge endcaps already discussed (Sect. 3.2)). An extra $I/2$ current line running in the opposite direction along both y-edges of the mirror, cancels the net current flow in the x-direction and approximately eliminates the perturbing B-field (see Fig. 1).

Additional stray B-fields arise from current leads connecting the mirror to a power supply. These leads could enter and exit the system from many directions; rather than investigating each, we present a simple mirror geometry that simultaneously adds the desired endcap currents on both the x and y mirror edges and minimizes all connecting lead stray fields. Figure 1 shows the idea, with the solid line representing the mirror circuit carrying current I and the two dotted lines representing lines of current $I/2$.

Finally we return to the waveguides mentioned at the end of Section 3.2. The existence of these guides is a manifestation of the finite mirror size. It is not our intention to discuss waveguides in this paper [28], but we do note briefly that one need not rely simply on the interference of the inherent finite-mirror $\mathbf{B}_{\rm e}(x,z)$ field with the infinite mirror harmonics; expressly applying an appropriate bias B-field in the x- or z-direction can form a much stronger/deeper series of waveguides [29].

3.5 Adding a holding field

To satisfy the adiabaticity assumption of Section 2, a "holding" bias field is required to prevent the total field vector (mirror+bias) from varying too rapidly in space. With endcaps employed along the mirror's y-edges, there are no appreciable B_y components anywhere near the mirror centre giving a free axis along which to apply the necessary orthogonal holding field, B_h. Unlike the stray fields above, no additional interference terms are introduced and the resultant field is simply B_h added in quadrature with the existing mirror field.

Apart from ensuring adiabaticity, the holding field also slightly modifies the turning height of an atom of given incident energy. This slight change can easily be compensated for by changing either the mirror current or the atom drop height. Therefore we consider the effects of B_h at a certain fixed turning height, noting that the associated incident velocity/mirror current may change slightly. We note first that addition of a holding field along a free axis does not alter the slope, $\mathrm{d}z/\mathrm{d}x$, of any iso-potential (the extra holding field reduces $\partial B/\partial x$ and $\partial B/\partial z$ equally). Nonetheless, the holding field can still affect the specularity of reflection. Close to the surface where the mirror B-field is large in comparison to the holding field, the reduction in $\partial B/\partial x$ and $\partial B/\partial z$ is negligible; further from the surface, where the mirror B-field is smaller, the reduction is greater. The spatially dependent reduction in $\partial B/\partial z$ can act to sharpen the potential, narrowing the height band in which an atom experiences appreciable forces and making the potential look slightly more "wall-like". Depending on where the turning point occurs, this "localization" can reduce the rms reflection angle despite there being no change in any individual iso-potential. Additionally, the reduction in $\partial B/\partial x$ reduces the transverse momentum imparted to the atom while essentially still in free fall.

4 Mirror specularity simulations

Since the reflecting mirror field is not a perfect "hard wall" potential, the atom experiences appreciable forces over some distance before turning and the imparted momentum depends on a weighted integral of the slopes of the iso-potential lines in the vicinity of the turning point. For a field given by (2), a multiplicative correction factor enables one to regard the reflection process as occurring off an equivalent "hard wall" potential [13]. Calculating the reflection angle then simplifies to determining the iso-potential slope at the turning point alone. However, if the turning point lies slightly further from the surface, equation (2) starts giving way to (5) and such a multiplicative factor no longer applies. The finite-size-induced roughness region can appreciably affect the atom's trajectory as it passes through, even if the atom does not turn near there. Additionally, applied holding fields can also affect the reflection angle. Therefore, to obtain accurate values for the optimum turning heights and for the rms deflection angles, θ_RMS, from perfect specular reflection, we perform a full numerical integration of the semi-classical atom trajectories through the mirror B-fields described above.

Results are quantified by averaging simulations over atoms dropped at varying x-positions (spanning a width $W/10$) about the mirror centre. Figure 5A shows θ_RMS for an odd mirror as a function of turning point height above the mirror surface for $B_\mathrm{h} = 0, 1$ and 10 gauss (in comparison with a 60 gauss surface field). Also plotted is an analytic calculation for an infinite mirror (assuming "hard-wall" potentials and including adjustment factors [13] for each Fourier harmonic present to account for the omitted averaging integration over iso-potential lines). Good agreement is seen close to the surface but, while the roughness of the infinite mirror decreases monotonically with height, the roughness of the finite mirror begins increasing beyond a certain optimum distance from the surface. To clarify the relative magnitudes of the contributions of different heights, z, to θ_RMS, Figure 5B shows the transverse momentum imparted to an atom (reflected 2.5 decay lengths from the surface) at each position during its fall. Since the atom spends most time near its turning point, the transverse momentum transfer should peak there. The curve's additional maximum though, is due to the strong gradients around the minima occurring in the finite mirror region around $z \approx a$. This maximum vanishes with increasing holding field as expected.

In Figure 5C, θ_RMS-turning point curves compare an odd mirror, an odd mirror with endcaps, and an odd mirror with endcaps and a wire profile determined by our optimization algorithm. All plots are calculated for an experimentally realistic $B_\mathrm{h} = 1$ gauss. The minimum θ_RMS value is 0.1 mrad [30] and occurs approximately 1.25 decay lengths from the mirror surface. Therefore, for this mirror the current required to reflect atoms with the maximum degree of specularity is given by $I_\mathrm{optimum} \approx I_\mathrm{threshold}\mathrm{e}^{1.25}$, where $I_\mathrm{threshold}$ is the minimum current required to reflect atoms. For example, for ^{85}Rb atoms (ground state $F = 3$, $m_\mathrm{F} = 3$) dropped from a MOT 2 cm above the mirror surface, a typical 1 cm^2 mirror ($a = 200$ μm , $N = 101$) with surface field per unit current B_0/I of order 60 gauss [17,18], has an $I_\mathrm{threshold} \approx 0.45$ A. This gives $I_\mathrm{optimum} \approx$ 1.5 A, a value considerably below the maximum current that can be pulsed through such a mirror. Even for the unoptimized odd mirror shown (rectangular wires and no endcaps), the minimum occurs below 2 decay lengths from the surface and at $I_\mathrm{optimum} \approx 3$ A, again below the maximum current achievable. In addition to decreasing the minimum θ_RMS, the θ_RMS-turning point curve (C) in Figure 5C exhibits a smaller curvature around its minimum, implying that a larger range of incident velocities can be simultaneously reflected with this higher degree of specularity. This robustness reduces constraints on the monochromaticity of the atomic ensemble to be reflected.

5 Conclusion

Unlike an infinite mirror, whose specularity increases monotonically as a function of reflection height above the surface, a finite mirror exhibits an optimal reflection

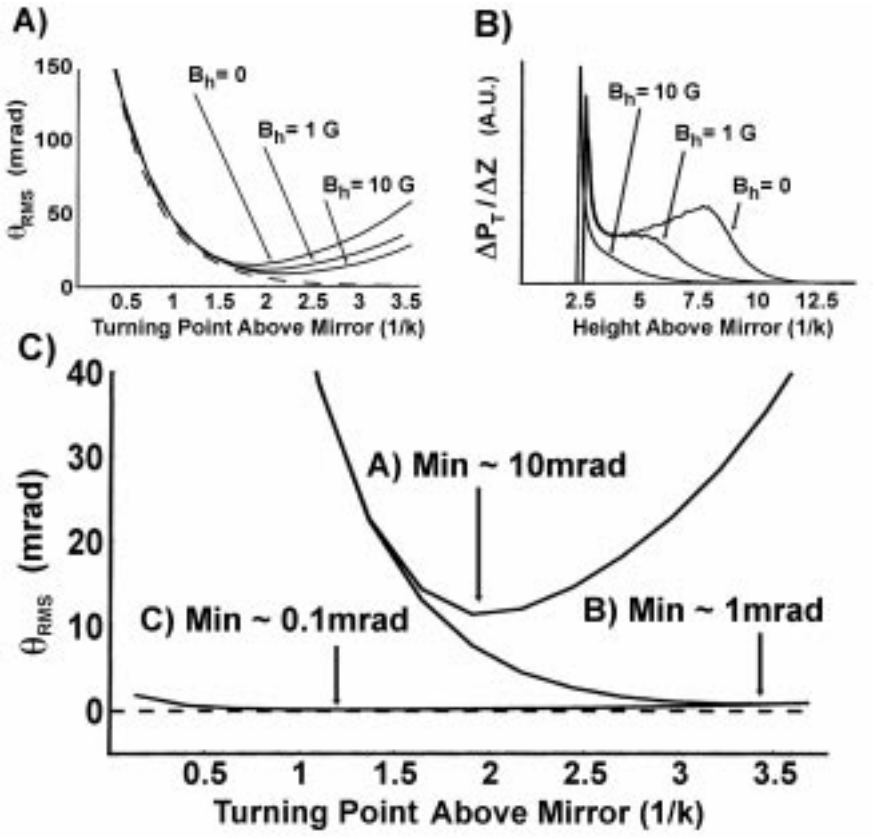

Fig. 5. Predicted curves of rms angular deviation from specular reflection versus atom turning point height above the mirror surface, showing an optimal turning height. Curves are for a 101-line mirror for various holding fields and are contrasted against the prediction for an infinite mirror (dotted line). (B) Transverse momentum imparted to an atom at each height through which it falls. Local maxima in the curves are due to strong field gradients around the minima in the absolute magnetic field caused by the finite mirror size. (C) Progressive smoothing of the mirror in going from (A), an odd mirror with wires of rectangular cross-section to (B), the same odd mirror but with correcting endcaps, and then (C), the odd mirror with correcting endcaps and an optimized wire cross-sectional profile. (An even mirror is omitted, it falling mainly off the scale of the graph.) The dashed line corresponds to perfect specular reflection ($\theta_{\rm RMS} = 0$).

height that maximizes the specularity. Notably, this optimum height can be reached (and exceeded) by available magnetic mirrors (both permanent and electromagnetic).

In this paper we have described how the wire cross-sectional profiles, the finite size, the even/odd number of current lines, and the holding field all affect the mirror's roughness. Based on these observations, we have considered possible means to reduce the rms angular deviation from perfect specular reflection to below 0.1 mrad and to increase the range of incident velocities which can simultaneously be reflected with greater specularity.

We have chosen an electromagnet mirror as our model system, it having the advantage of an experimentally easily tunable field strength, but analogues of the results apply equally well for the static permanent magnet mirrors. Whether using current-carrying wires or permanent magnets, the use of an appropriate number of elements, endcaps, and optimized magnetization profiles appears a possible promising route towards highly specular atom mirrors.

The authors thank A. Aspect, L. Cognet, P. Featonby, C. Lee, M. Olshanii, W.D. Phillips, V. Savalli and C. Westbrook for useful discussions. This work was supported by National Science Foundation Grant No's: PHY9312572, PHY9732449, and DMR9400396. JHT acknowledges support from the Fannie and John Hertz Foundation.

References

1. A. Landragin, G. Labeyrie, C. Henkel, R. Kaiser, N. Vansteenkiste, C.I. Westbrook, A. Aspect, Opt. Lett. **21**, 1591 (1996).
2. C.S. Adams, O. Carnal, J. Mlynek, Adv. At. Mol. Opt. Phys. **34**, 1 (1994).
3. V.I. Balykin, V.S. Letokhov, Appl. Phys. B **48**, 517 (1989).
4. M. Wilkens, E. Goldstein, B. Taylor, P. Meystre, Phys. Rev. A **47**, 2366 (1993).
5. U. Janicke, M. Wilkens, Adv. At. Mol. Opt. Phys. **41**, 261 (1999).
6. R.J. Cook, R.K. Hill, Opt. Commun. **43**, 258 (1982).
7. V.I. Balykin, V.S. Letokhov, Yu.B. Ovchinnikov, A.I. Sidorov, Phys. Rev. Lett. **60**, 2137 (1988).
8. M.D. Kasevich, D.S. Weiss, S. Chu, Opt. Lett. **15**, 607 (1990).
9. H.J. Lee, C.S. Adams, M. Kasevich, S. Chu, Phys. Rev. Lett. **76**, 2658 (1996).
10. G.I. Opat, S.J. Wark, A. Cimmino, Appl. Phys. B **54**, 396 (1992).
11. T.M. Roach, H. Abele, M.G. Boshier, H.L. Grossman, K.P. Zetie, E.A. Hinds, Phys. Rev. Lett. **75**, 629 (1995).
12. I.G. Hughes, P.A. Barton, T.M. Roach, M.G. Boshier, E.A. Hinds, J. Phys. B **30**, 647 (1997).
13. I.G. Hughes, P.A. Barton, T.M. Roach, E.A. Hinds, J. Phys. B **30**, 2119 (1997).
14. A.I. Sidorov, R.J. McLean, W.J. Rowlands, D.C. Lau, J.E. Murphy, M. Walkiewicz, G.I. Opat, P. Hannaford, Quantum Semiclass. Opt. **8**, 713 (1996).

15. D. Meschede, I. Bloch, A. Goepfert, D. Haubrich, M. Kreis, F. Lison, R. Schütze, R. Wynands, in *Atom Optics*, edited by M. Prentiss, W.D. Phillips, *SPIE Proceedings* **2995** (SPIE-International Society for Optical Engineering, Berlingham, WA, 1997), p. 191.
16. D.C. Lau, A.I. Sidorov, G.I. Opat, R.J. McLean, W.J. Rowlands, P. Hannaford, Eur. Phys. J. D **5**, 193 (1999).
17. M. Drndić, K.S. Johnson, J.H. Thywissen, M. Prentiss, R.M. Westervelt, Appl. Phys. Lett. **72**, 2906 (1998).
18. K.S. Johnson, M. Drndić, J.H. Thywissen, G. Zabow, R.M. Westervelt, M. Prentiss, Phys. Rev. Lett. **81**, 1137 (1998).
19. V.V. Vladimirskiĭ, Sov. Phys. JETP **12**, 740 (1961).
20. Recent experiments conducted at the Institut d'Optique (Orsay, France) have since verified the predictions made here of an optimal turning height and an even/odd parity effect.
21. The B-field above a mirror of circular cross-sectional wires is easily calculable by noting that it is the same as that for a mirror of delta-function point wires – the surrounding Amperian loops map identical fields for both systems.
22. We also assume atoms with sufficiently large magnetic moments/small incident energies such that required reflecting field strengths are small and the potential depends only linearly on the B-field magnitude (linear Zeeman regime). Quantitative changes to results quoted here may be needed if stronger reflecting B-fields are required.
23. An alternative transition height is the start of the second region (rather than its middle) and can be approximated as that where the additional line's contribution is of similar magnitude to the B-field roughness, rather than to the B-field magnitude itself. This implies equating the current line B-field to the second term in (2) (normally the leading roughness term). The exact transition height can then vary substantially through its dependence on the wire profiles.
24. The finite mirror line y-length also introduces curvature into the B-field. This curvature depends on N, L, a, and the distance from the mirror centre. Provided the distance from the centre is small (for example, $y = 1$ mm in a typical 100/101 line 1 cm^2 mirror ($L = 1$ cm, $a = 200$ μm)) the curvature at all heights of interest can be shown negligible compared to other roughness contributions.
25. For wires of assumed homogeneous material, current density variations arise through temperature-dependent changes in local resistivity due to ohmic heating. For small wires though, even a single degree change across the wire would result in unphysically large temperature gradients being established. For example, for a typical 10 μm high, 100 μm wide gold wire carrying a 1 A current, the relevant heat equation yields a maximum temperature difference across the wire of one part in 10^4 to 10^5, limiting any spatial variations in resistivity/current density accordingly.
26. As Sidorov *et al.* note, second order endcap correction is achieved by placing the endcap wires at precisely $a/4$, instead of the mirror wire spacing $a/2$, from the mirror edge.
27. In this paper we assume perfect mirror manufacture. However, imperfections in mirror manufacture can also be modeled as additional intrinsic stray/error fields interfering with the infinite mirror harmonics. Fortunately, the same total current flows everywhere in the series mirror circuit, reducing effects of manufacture error.
28. J.H. Thywissen, M. Olshanii, G. Zabow, M. Drndić, K.S. Johnson, R.M. Westervelt, M. Prentiss, Eur. Phys. J. D **7**, 361 (1999).
29. Recently, E. Hinds has independently suggested an alternative means, combining magnetic and electric forces, to create a similar series of waveguides: E.A. Hinds, in *New Directions in Atomic Physics*, edited by C.T. Whelan (Plenum, in press).
30. $\theta_{\rm RMS}$ of 0.1 mrad could be further reduced if a larger holding field were applied, or if higher order correcting endcaps were used. Second order (x-edge) endcap correction can reduce $\theta_{\rm RMS}$ to a few μrad. However, we show only first order endcap calculations, since other, previously negligible, higher order effects dominate before reaching this μrad level.